Terrain and soil influences on ERS-1 SAR image

T.K. Alexandridis[1], C.A. Bird[2], T. Mayr[2], G. Thomas[3], and E. Stavrinos[4]

[1]School of Agriculture, Aristotle University of Thessaloniki, 54124 Thessaloniki, Greece (e-mail: thalex@agro.auth.gr).
[2]Natural Resources Department, Cranfield University, United Kingdom.
[3]Queen Mary College, University of London, United Kingdom.
[4]Directorate of Water Reclamation and Soil-Water Resources Planning, Ministry of Rural Development and Food, Greece

The increasing availability of synthetic aperture radar (SAR) remote sensing imagery for agricultural and soil science applications has created the need for a better understanding of how SAR relates to the specific features on the earth's surface. In this study, several terrain and soil parameters that were known to influence the radar return signal were measured or estimated, and with the use of calibrated ERS-1 SAR imagery, the relationships and the amount of influence on the radar return signal were investigated. The study area was an agricultural region of Bedfordshire and all the test sites were bare fields at the time of image acquisition. The results reveal that the parameters that influenced the signal significantly were the surface roughness, the local incidence angle, the tillage direction and the soil moisture content. In contrast, the parameters slope and aspect showed little to no influence. However, the relations were medium to weak, probably due to constrains in sample size and specific conditions of the study area.

***Index Terms*— Remote sensing, Synthetic Aperture Radar, Radar signal analysis, Radar terrain factors, Soil**

I. Introduction

MICROWAVE (radar) remote sensing has a long history, which has largely been supported by airborne campaigns, and only recently by satellite sensors (e.g. SEASAT, 1978). Microwave remote sensing is highly promising due to the advantage that radar are 24 hours, all weather operation systems. They have thus been used to study areas frequently cloud covered, such as the Amazon rain forest [1], or during the monsoon season [2], which would have been prohibitive with optical sensors.

Radar images have different characteristics to those produced by optical sensors. Images derived from optical sensors are recordings of the intensity of reflection or emittance of sunlight and the earth's radiation. Microwave images, however, are influenced by a great number of other parameters, in a more complicated and not very well known way. Their ability to detect smooth water surfaces from rough land has been utilized in hydrological and environmental studies, such as identification of inundated vegetation [3], mapping wetland habitats [4], identification of oil spills [5], and delineation of aquacultures [6, 7]. Their distinctive characteristics have also been useful in agricultural and soil science studies, detecting the extents of flooded cropland [8], identifying the main types of rice cultivation practices [9], mapping degraded soils [10], deriving information for topsoil moisture content and surface roughness [11], and mapping agricultural crops [12, 13].

Radar imagery has two proposed advantages in studying soil properties over the optical systems. First, radar images can be obtained independent of weather conditions, which render them ideal during the frequently cloud-covered late autumn studies, when crops are harvested and soil related information is easier to be collected with remote sensing. Second, the nature of the radar being volume scattered and its ability to penetrate in the soil is thought to give better results for soil surveys than optical sensors, since the latter only reflect the properties of the top few micrometers of the soil surface, which are clearly not representative of the soil profile.

However, a number of other parameters influence radar backscatter (the radar return signal), and are not well understood, in contrast to the optical wavelengths. Parameters related to topography are the terrain slope, aspect and the local angle of incidence of the incoming beam. A simplification of topographically induced radiometric distortions in SAR imagery is an increase in σ^o (backscattering coefficient) on slopes facing the radar, and a decrease in σ^o on slopes facing away from the radar. In the same way, slopes having a low incidence angle give a higher return signal than slopes having a higher incidence angle. It has been demonstrated [14] that σ^o of SEASAT imagery is dependant on topography, a relation that is reduced if the images are radiometrically corrected using a DEM. Reference [15] based on SEASAT data concluded that the geometric parameter revealing the strongest influence in σ^o is the local angle of incidence, and suggested a simple correction function based on the calculation of the mean grey value for each incidence angle class. Reference [16] showed that an increase in moisture content either of soil or vegetation causes an increase in the electrical conduction properties of the medium (permittivity) which in turn influences the degree of backscattering of microwave radiation, resulting with a brighter return signal. Finally, the tillage row direction is an important influencing parameter to ERS-1 SAR images according to [17], who demonstrated that fields with tillage row direction perpendicular to the satellite look direction scatter more energy back towards the sensor than will fields with row directions parallel to the look direction, decreasing the images' ability to detect other soil properties. Hence, it may be difficult to derive a clear indication for soil properties, a valuable input to several applications of resources mapping and management (soil mapping, wetland assessment, etc.).

The aim of this work was to investigate the level of influence of radar return signal to several terrain and soil

parameters, which may hinder the use of radar images in soil surveys. To achieve this, ERS-1 SAR images were used and the parameters were measured during field survey or estimated using models. Finally, statistical analysis has revealed the amount of soil related information that can be extracted from SAR images.

II. Materials and Methods

A. Description of study area

The study area is located in Bedfordshire (UK), it covers 100 km2, stretching from Biggleswade westward, to the outskirts of Bedford, including part of Sandy (Fig. 1). The centre co-ordinates are N 52° 5', W 0° 19'. Most of the land is cultivated and includes traditional market gardens on the Ivel terraces. The immediate area around Biggleswade is noted for the production of Brussel sprouts. In the west the soils are heavier and the land is largely under cereal production. Woodland occurs mainly as a discontinuous band running north-south through the centre of the district often on the heavier, more intractable clay soils and least productive Greensand soils [18].

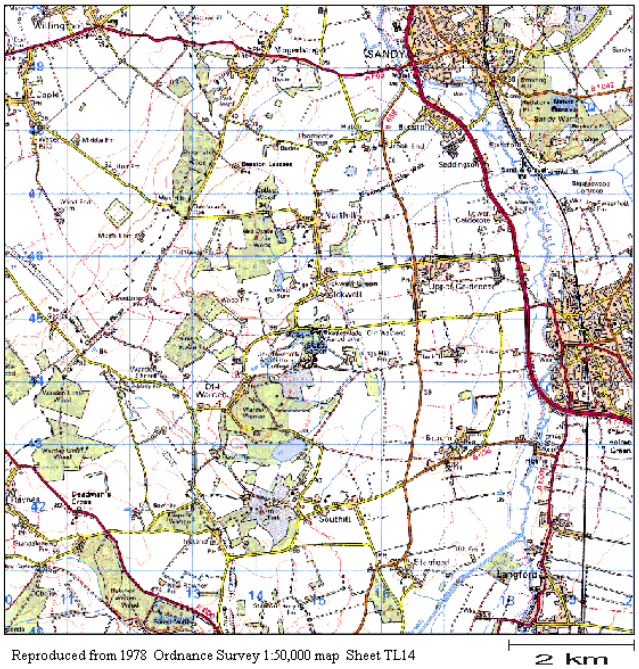

Fig. 1. Topographic map of the study area (source: Ordnance Survey).

The district is underlain by lower Cretaceous and upper Jurassic rocks, which are mostly masked by Quaternary drift deposits. The Cretaceous strata consist of the Gault and Lower Greensand, while the Jurassic rocks are represented by Ampthill Clay and Oxford Clay. The local Quaternary deposits vary widely in lithology, appearing mostly as gravel and sand deposits, probably from glaciofluvial origin. Recent deposits are represented by a broad strip of alluvium in the Ivel valley, which is mostly silty clay, in places interbedded with peat [18]. A full description can be found in [19].

A wide variety of soil series exist in the Biggleswade area. They belong to the brown earth or pelosol group and some to the stagnogley group. Some, close to Ivel are alluvial and earthy peat soils. The soil series classification together with the soil groups are summarised in Table I.

TABLE I
Classification of Soil Series in the Study Area

Code	Group
3.7	Rendzina-like alluvial soils
4.1	Calcareous pelosols
4.3	Argillic pelosols
5.1	Brown calcareous earths
5.4	Brown earths
5.5	Brown sands
5.7	Argillic brown earths
5.8	Paleo-argillic brown earths
7.1	Stagnogley soils
8.1	Alluvial gley soils
8.5	Humic-alluvial gley soils
10.2	Earthy peat soils

The relief is mild and the slopes are mainly gentle. The highest point is 90 m above mean sea level, north of Warden Little Wood on a broad plateau formed in chalky till. The main valley is formed by River Ivel, which flows northwards where the lowest point of the study area lies, at 21 m.

B. Field survey

The study area was surveyed from the 28th May to 31st May 1996. The aims of the field survey were to identify the bare fields, to perform several parameter measurements, and to identify sites that might help the geometric correction of the satellite imagery. Ordnance Survey (OS) 1:10,000 maps were used (Sheets TL14) and land use was marked onto them by visual inspection.

It was decided that only bare fields or crops that were beginning to emerge would be useful in this study. Vegetated sites were avoided as the scattering mechanism is too complex [20]. Therefore, from the bare fields that were identified, a sample of 32 fields, evenly distributed across the study area was selected (Fig. 2). On these fields, surface roughness and tillage direction were measured during field survey.

C. Satellite image acquisition and processing

An ERS-1 SAR image (Precision Subscene - PSn) was acquired (21 May 1996), covering an area of 25x25 km, at a 12.5m spatial resolution (ground sampling distance). The SAR image was selected to be contemporary with the field survey.

Accurate radiometric calibration and across track balancing is required for the radar images, to enable the derivation of backscattering coefficients σ^o, and successfully relate σ^o to soil conditions [16]. This was performed using the formulae presented in [21], which take into account the earth curvature

and radar local depression angle. However, no radiometric correction for the topographic effect was performed, so that the influencing factors related to topography would not be eliminated.

The σ^o image was registered with the local depression angle layer and geometrically corrected using 14 ground control points, evenly distributed around the study area. Their coordinates were identified on a 1:10,000 OS map. The RMS error was estimated to be 4.22 pixels (x: 3.76, y: 1.92). The RMS x co-ordinate was much bigger due to the inherent distortion in the radar range direction. At the end, the image was resampled to a 15m pixel with the nearest neighbour algorithm so that the original values would be preserved.

Speckle suppression is an important processing that must be applied to radar imagery. This not only helps the data achieve a normal distribution, but also clears the image of unreal values and gives a better visual appearance [22]. Several filters were tested on the σ^o image (local region, Lee, Lee sigma). Finally the Lee sigma was applied once, as it provided the optimum balance between noise removal and elimination of high frequency information, based on visual assessment (Fig. 2).

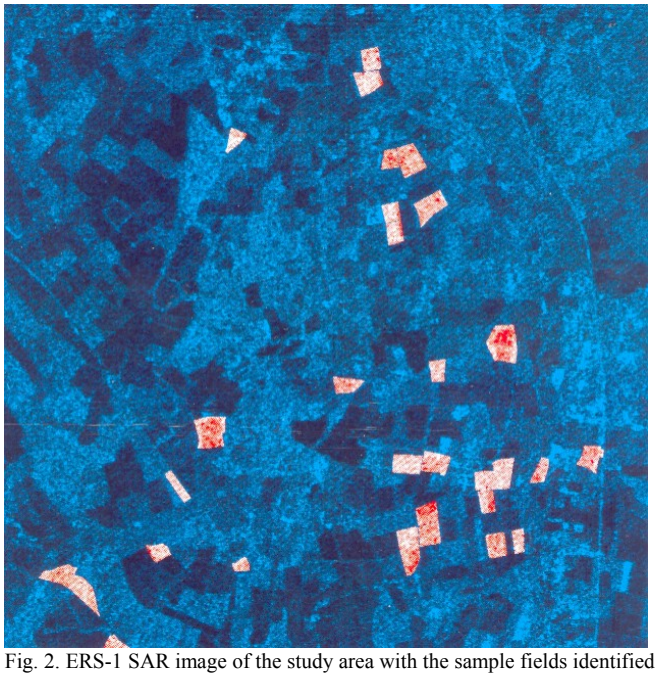

Fig. 2. ERS-1 SAR image of the study area with the sample fields identified in red.

D. Terrain parameters

1) Digital Elevation Model

Height observations on a 100 metre grid were used to create a DEM (Fig. 3a). These sparse data were considered satisfactory for this study area as the relief is of no particular undulation. However, they were not dense enough to measure the convexity of the slopes. The following parameters were estimated from the DEM, using spatial analysis routines in a GIS:

- percentage slope (Fig. 3b). The output values were classified to integers. The slopes in the study area ranged only from 0 to 22%.
- aspect relative to north (degrees) (Fig. 3c). A value of 0 is given to a north facing slope and a value of 360 is given to a pixel with no slope (and therefore no azimuth).
- aspect relative to range direction (103°) (degrees). This was calculated from the absolute value of the difference δ = range azimuth - terrain aspect. Therefore, a slope facing towards the radar would have a value lower than a slope facing away from the radar. This parameter was considered to describe the terrain aspect in an alternative way.

2) Slope at radar look direction (range)

For each pixel of the slope raster, the slope in the satellite look azimuth (range) was calculated using the following equation:

$$S' = S \cos(\delta)$$

where: S' is the slope at the satellite look direction (range), S is the maximum slope calculated by GIS spatial analysis, and δ = range azimuth - terrain aspect.

The values of the resulting raster ranged from -11.75 to7.95 %. The negative values were accepted, although they may seem unreasonable for a slope, as they represented slopes facing away from the radar. These slopes were expected to have a low return signal, while slopes with a high positive value were expected to have a stronger signal (Fig. 3d).

The slope at radar look direction was used to determine and mask out layover effects. Layover occurs at slopes facing the radar, when the terrain slope is steeper than the line perpendicular to the direction of the radar pulse, expressed by its depression angle. Thus, the following equation was used to mask out pixels where:

$$S' > \tan(90-\theta)$$

where θ is the local depression angle. No areas appeared to suffer from layover effects in this area of relatively low relief.

(a)

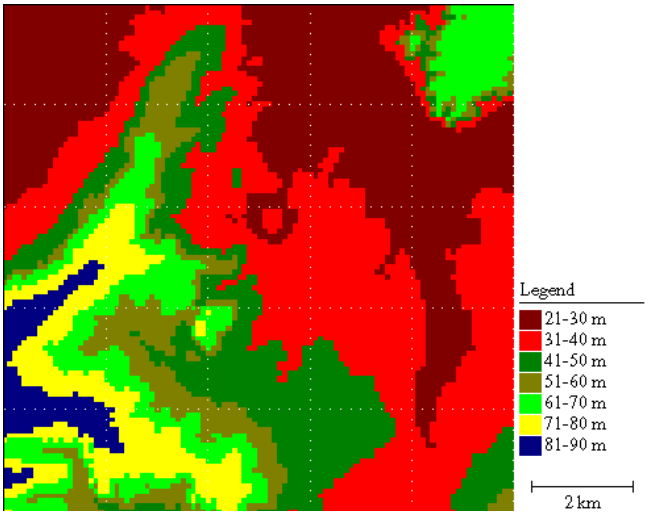

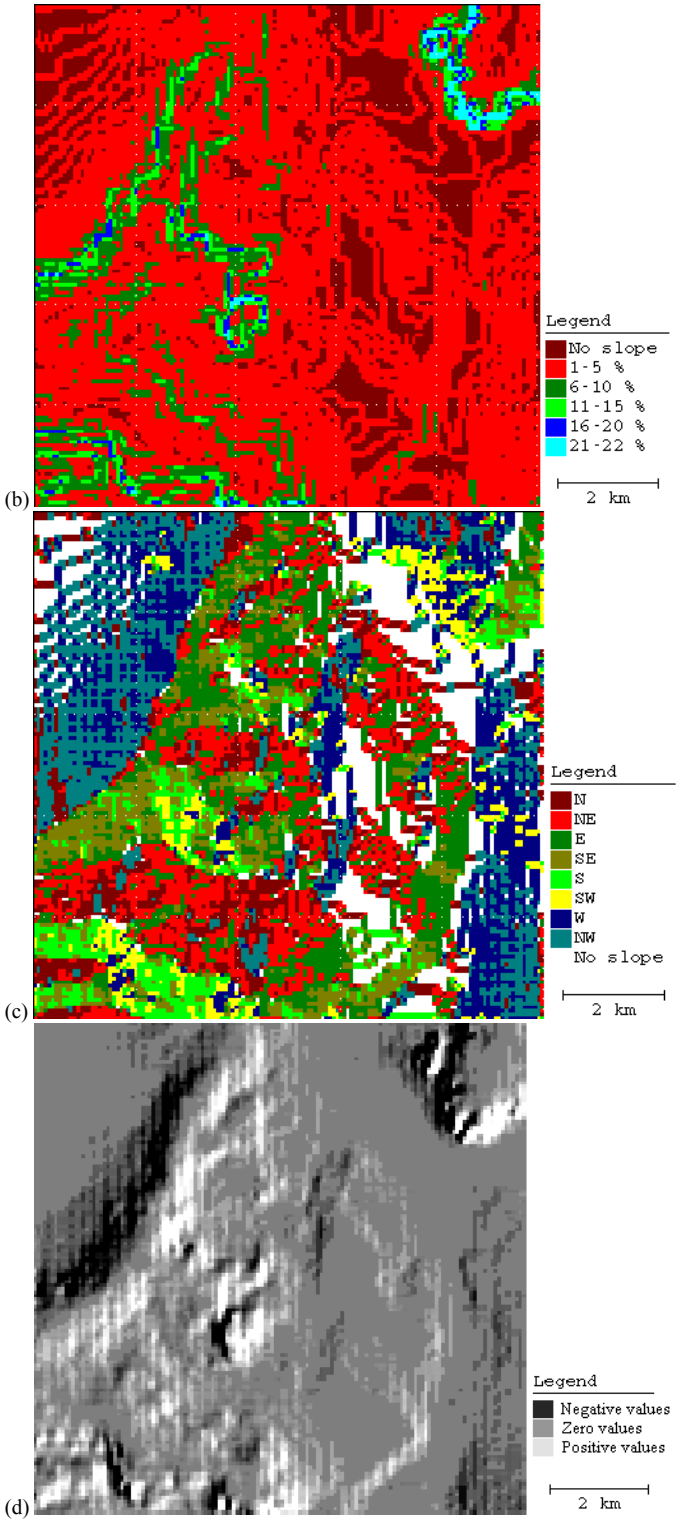

Fig. 3. Terrain parameters in the study area: (a) DEM, (b) percentage slope, (c) aspect relative to north, and (d) slope at range.

3) Local incidence angle

The local incidence angle (I) is the angle between the incident radar beam at the ground and the normal to the ground surface at the point of incidence (Fig. 4). In order to calculate this for each pixel of the DEM, the following formula was used [14], taking into account the terrain slope as well as the local depression angle:

$$I = \arccos\left(\cos\alpha \cdot \cos\theta + \sin\alpha \cdot \sin\theta \cdot \cos\gamma\right)$$

where: I is the local incidence angle, α is the slope (in degrees), θ is the depression angle, γ = beam azimuth - terrain aspect.

The local depression angle was calculated using the complex geometric formulae given in [21]. These formulae take into account the earth curvature and the pixel's position in the image swath.

The values of the resulting local incidence angle were ranging from 69.05 to 81.74 degrees. Low values represented locations of high slope or facing the sensor, while higher values represent locations of lower slope or facing away from the sensor.

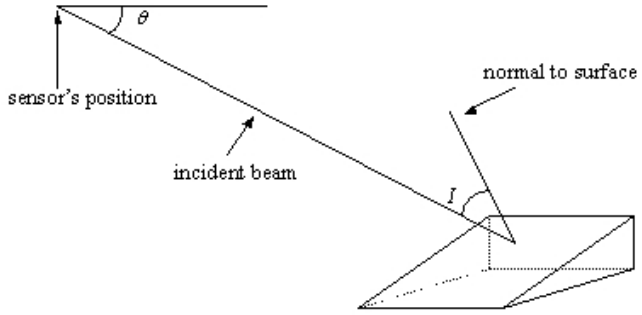

Fig. 4. Radar beam geometry.

E. Soil surface roughness

According to [11], it appears in the radar images that it is the land use that is recorded and not the different soil types or variations in the soil moisture content. However, it is the surface roughness which dominates the radar response, thus fields could be clearly identified because it is the type of crop and the stage of crop growth, or in case of bare field it is the soil surface roughness, which is recorded on the radar image.

The tillage row direction was measured during field survey for the furrowed fields only, since the flat fields did not have a distinct tillage direction. In these fields there were recently created ridges for potato sowing. The azimuth of the tillage direction from north was recorded using a simple surveying compass. In the statistical analysis, the difference of the tillage direction azimuth from the satellite look (range) direction was used (tillage direction relative to range), as it was thought that would describe in a better way this parameter.

Also, small scale roughness measurements were taken in 32 sites during the field survey. These were bare fields, or fields sown with summer crops that were beginning to emerge. For each site two or three point measurements were conducted, depending on their homogeneity, in the corner of each field, in order not to disturb the germinating crops.

At each measurement point, a 1 m ruler was placed gently on the soil surface so that it rested on the highest points, aligned with the radar look direction. Measurements for two radar look directions were taken, (azimuth 103° and 257°) for descending and ascending orbits respectively, as it was not known at that time which image would be used for final analysis. The vertical distance between the ruler and the soil

surface was measured at eleven points, 100 mm apart. The mean surface height and the standard deviation were calculated and the point measurements for each location were averaged, to give a value for the whole field, based on the method described in [11]. The standard deviation cannot provide a complete characterisation of surface roughness, but an adequate measure for comparing relative roughness. In this way, the random roughness of soil clods formed by the combined action of the tillage practice, natural soil aggregation and weathering is defined, which can describe the small scale roughness. Unfortunately, the periodic patterns of tillage and row structure are not described with these measurements [23].

F. Soil moisture estimation

The sensitivity of backscatter to soil moisture is well known [20]. Radar response is also dependent on the dielectric properties of the soil, which fluctuates according to the soil water status. Soil moisture is also a factor that limits the signal penetration to a few centimetres, in very wet soils. However, penetration is also dependent on the radar wavelength. For C band wavelength the radar signal penetrates average wet loams about 20-30 cm [22]. It was therefore decided that the soil moisture should be calculated for the top 25 cm.

Soil moisture was estimated using the BALANCE model [24]. This model estimates the soil moisture balance at a given date by measuring the gain (irrigation and precipitation) and the loss (evapotranspiration). Inputs for the model were:

- Meteorological data for the period 23/12/95 to 30/5/96, collected from the Shuttleworth weather station, lying in the middle of the study area. Lack of other meteorological stations operating in or near to the study area prevented spatial interpolation.
- Soil data, such as topsoil depth, volume water fraction in various conditions, total available water, soil evaporation characteristics and drainage characteristics. From these, the first three were available for each soil type by the data bank of Soil Survey and Land Research Centre (SSLRC). Default values given by the program were used for the soil evaporation characteristics (as it is difficult to measure). The drainage characteristics had been calculated by SSLRC as follows: Pedo-transfer functions were used to calculate the soil water release curve based on the soil texture. The hydraulic conductivity function was calculated using Van Genuchten equations, which allowed the calculation of the drainage factor.

It was assumed that all the soils were saturated on the 23rd December 1995 since 52.1 mm precipitation had occurred over the past three days. The BALANCE program was used for the dates from 23/12/95 to 21/5/96.

The estimated soil moisture values were relatively high (slightly lower from the field capacity), which could be due to the formation of a dry layer of 2-3 cm on the soil surface, which hindered evaporation of the rest top soil water.

Clearly this soil moisture estimation for the bare fields of the study area was a function of the soil type. This is not always the case, as it depends also on the micro-climate of the area, as well as the past tillage and irrigation conditions, which are unknown.

III. RESULTS

Results from the measurement or modelling of the previously mentioned parameters were added as information layers in a GIS. The sampling of σ^o on the radar image was based on area averaging to avoid the influence of speckle, and pixels close to the fields' boundaries were excluded to avoid errors due to edge contamination and registration mismatch. Therefore, the mean values calculated within each of the 32 fields were the dataset used as an input to the statistical analysis to identify the relations between the image values and the various parameters. The mean and standard deviation for each parameter in the recorded dataset is provided in Table II.

TABLE II
DESCRIPTIVE STATISTICS OF THE SAMPLED PARAMETERS

Layer name	min.	max.	mean	st.dev.
Backscattering coefficient (dB)	-30.87	18.68	-12.67	3.79
Local incidence angle (deg.)	62.04	81.73	69.78	0.98
Slope (%)	0	22	1.26	1.96
Slope at range (%)	-11.74	7.95	0.03	0.96
Aspect rel. to north (deg.)*	-179	180	-	-
Aspect rel. to range (deg.)	8	98	-	-
Soil moisture (% vol.)	18.1	40.8	-	-

* 360 denotes no slope

The recorded samples in the 32 locations were used as an input to regression analysis between the image values (filtered backscattering coefficients) and each one of the parameters (Fig. 5).

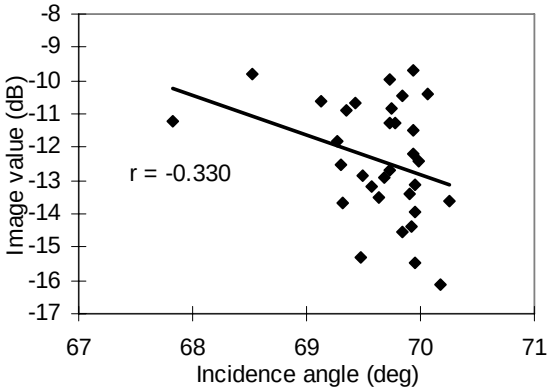

(a)

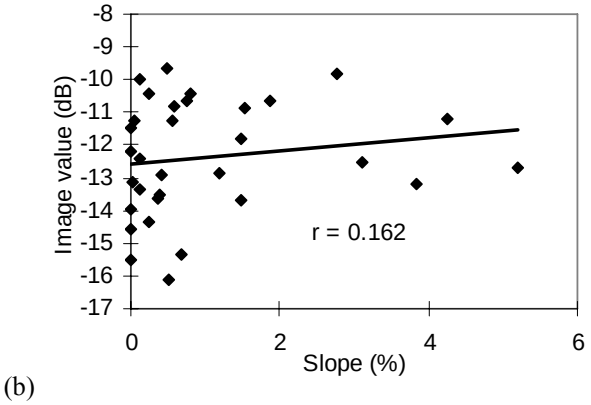

(b)

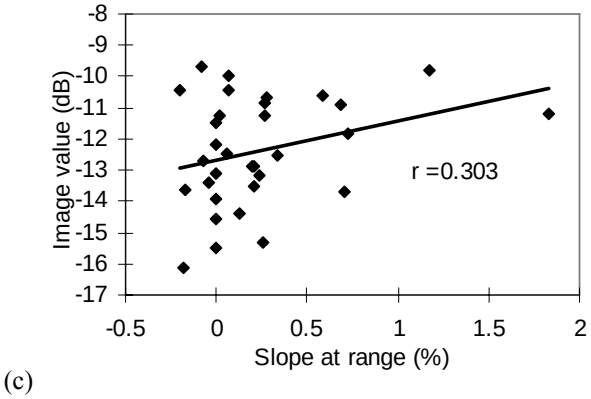

(c)

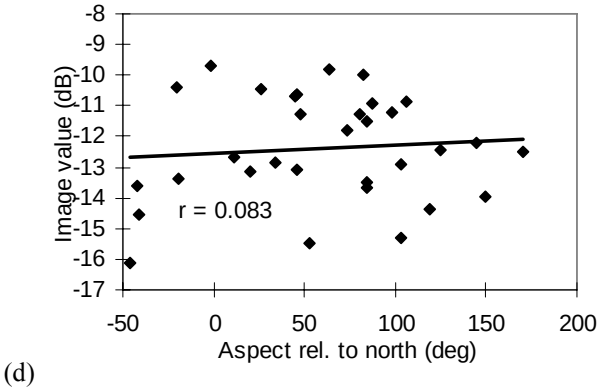

(d)

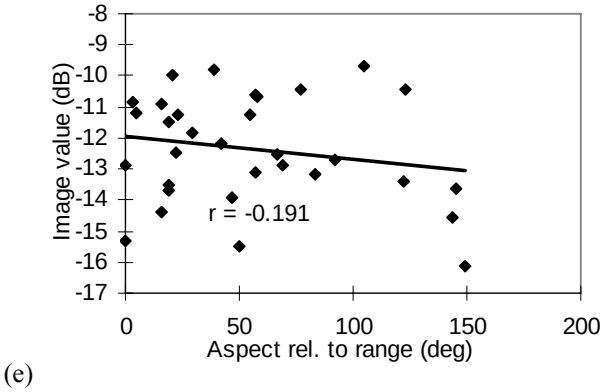

(e)

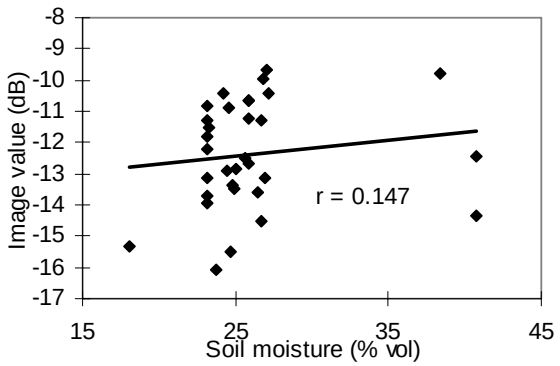

(f)

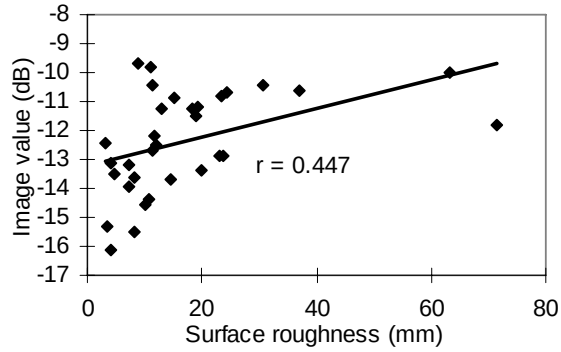

(g)

Fig. 5. Scatter plots of σo with the investigated parameters for all sampled fields: (a) incidence angle, (b) slope, (c) slope at range, (d) aspect rel. to north, (e) aspect rel. to range, (f) soil moisture, and (g) surface roughness.

Within the samples, two categories were considered: flat and furrowed fields. The sampled furrowed fields, though they were small in number had a different behaviour, especially regarding the surface roughness. Another reason for the division was the tillage row direction measurements that were conducted on the furrowed fields. Therefore, a separate regression analysis was performed with the two categories. The correlation coefficients are listed in Table III.

The parameters: aspect relative to north, aspect relative to range, soil moisture and slope have little to no influence on the backscatter variations. However, the local incidence angle, the slope at range and especially the surface roughness have a clear influence on the variation of the radar signal. These parameters have the relationship expected (according to background) with the image values: positive for slope at range and surface roughness, and negative for the local incidence angle.

Dividing the sample into the two categories, the relationships for the flat fields have the same expected sign. It is worth noting the increase of the correlation coefficient between σ^o and soil moisture from 0.147 to 0.316.

For the furrowed fields, the parameters aspect relative to north and aspect relative to the range show very little influence. On the other hand, the parameters tillage direction relative to range, local incidence angle and soil moisture show a higher relation with σ^o. The positive relationship of tillage direction relative to range with σ^o was expected, since low values of the former mean ridges parallel to the radar beam

direction, and therefore lower return. This time though, the relation of σ^o with aspect relative to north, aspect relative to range and soil moisture is inverted. This negative relationship of σ^o with the soil moisture does not agree with results recorded in previous studies [23].

It is noted that the investigated parameters do not always show a normal distribution. Transformation to logarithmic scale was tried unsuccessfully, due to the negative values of some parameters. This fact should be considered in the interpretation of the results of the statistical analysis.

The correlation coefficients showed weak to medium values, but some were statistically significant and highly significant, meaning that within the population of bare fields in the study area σ^o is related to the parameter in question (Table III). The correlation coefficients indicate the different significance of the various parameters to the variation of the image values. In future communication, in depth statistical analysis will give insight to the individual relations of the parameters with σ^o.

TABLE III
CORRELATION COEFFICIENTS (r) BETWEEN σ^o AND THE INVESTIGATED PARAMETERS

Parameter	All fields (32 samples)	Flat fields (27 samples)	Furrowed (5 samples)
Incidence angle	-0.330 *	-0.310	-0.829 *
Slope	0.162	0.127	0.726
Slope at range	0.303	0.289	0.739
Aspect rel. to north	0.083	0.129	-0.458
Aspect rel. to range	-0.191	-0.251	0.164
Tillage direction rel. to range	-	-	0.961 **
Soil moisture	0.147	0.316	-0.850 *
Surface roughness	0.447 **	0.550 **	0.797

* significant (at the 5% level)
** highly significant (at the 1% level)

IV. DISCUSSION

The parameter surface roughness shows the best correlation with the backscattering coefficient and describes 20% of the image values variance. When combined with soil moisture and local incidence angle, the three parameters together describe about 30%. Indeed, these three parameters were expected to influence the radar return more than all the rest, according to previous studies [14, 16, 17].

When dividing the sample into the two categories, there was a notable difference in the correlation coefficients. The increase in the relationship of soil moisture with σ^o in the flat fields could be due to the fact that soil moisture evaporates in a different way from flat than from furrowed fields, as the exposed surface changes. As expected, the relation of σ^o with surface roughness has increased when the sample was divided, since it was the major parameter in which the two samples were different.

For the flat fields only, the parameter surface roughness reveals the best relation with the image values and explains more than 30% of the variance. In combination with soil moisture and local incidence angle, the three parameters together describe almost 45% of the variance of σ^o.

In the case of the furrowed fields, the tillage direction relative to range explains more than 92% of the image values variance, and as a combination with the soil moisture and the local incidence angle they reach 100% (total variance). The fact that the relationship of σ^o with topsoil moisture is inverted in the case of the furrowed fields is difficult to explain. In fact, it is unsafe to conclude that the division into the two categories has improved the relationships, or has just excluded a potential distortion brought by the furrowed field samples.

It is evident that the relations of σ^o with the parameters are improved when the sampled fields were divided in two categories. It is unsafe though to discuss about inverting the equations and estimating parameters using ERS-1 images, even in case of the surface roughness. Such conclusions would be more valid with a larger sample size.

A. Limitations

The statistical relationships presented in the previous paragraph are, however, weak. This could be due to the design of the experiment, having a limited sample size, using a relatively coarse DEM and employing models for the estimation of soil moisture.

An important issue is that not all fields were bare at the time of image acquisition, which limited the potential of sample size. This was the only factor limiting the sample size, and therefore reducing the statistical significance of the results.

Also, there is great uncertainty in the estimation of the topsoil moisture, since different soil parameters (field capacity, permanent wilting point, bulk density, etc.) were used for the estimation of the drainage factor and the soil moisture content. The origin of the dataset used in the calculation of the drainage factor is from agricultural soils only, while the dataset used for the soil moisture estimation came from many types of land use. Additionally, the dataset used for the soil moisture estimation was derived from field measurements, while the other was estimated from accurate models.

Finally, the DEM grid was proven to be inaccurate in describing the slight variations in slope and aspect of the fields, which were mainly found on gentle to level terrain. This, in conjunction with the limited bare soils influenced the effect of topography on σ^o.

V. CONCLUSION

In this study, a number of parameters (local incidence angle, slope, slope at range, aspect relative to north, aspect

relative to range, soil moisture, surface roughness and tillage direction) that were known to influence the radar return signal (σ^o) were measured or estimated. The relationship of each one of them with the backscattering coefficients derived from an ERS-1 SAR image was tested with linear regression.

The results reveal that the parameters that influence σ^o significantly were the surface roughness, the local incidence angle, the tillage direction and the soil moisture content. In contrast, the parameters slope and aspect showed little to no influence. However, the relations were medium to weak, probably due to constrains in sample size and specific conditions of the study area.

The findings of this work can provide useful information for resources assessment in several studies, such as soil mapping, soil quality assessment, wetland assessment, environmental impact assessment, rural development support, precision agriculture, etc.

Despite the limitations, this study has provided a useful basis for further research into understanding how soil and terrain parameters influence radar images. Future work could study the parameters during autumn when bare soil exposure is maximum, in order to obtain a larger sample size and increase the validity of the conclusions.

REFERENCES

[1] J.-M. Martinez and T. Le Toan, "Mapping of flood dynamics and spatial distribution of vegetation in the Amazon floodplain using multitemporal SAR data," *Remote Sensing of Environment*, vol. 108, pp. 209-223, 2007.

[2] M. L. Imhoff, C. Vermillion, M. H. Story, A. M. Choudhury, A. Gafoor, and F. Polcyn, "Monsoon flood boundary delineation and damage assessment using space borne imaging radar and Landsat data," *Photogrammetric Engineering & Remote Sensing*, vol. 53, pp. 405-413, 1987.

[3] K. Jones, Y. Lanthier, P. van der Voet, E. van Valkengoed, D. Taylor, and D. Fernández-Prieto, "Monitoring and Assessment of Wetlands using Earth Observation," presented at GlobWetland: Looking at Wetlands from Space, Frascati, Italy, 2006.

[4] T. K. Alexandridis, E. Lazaridou, A. Tsirika, and G. C. Zalidis, "Using Earth Observation to update a Natura 2000 habitat map for a wetland in Greece.," *Journal of Environmental Management*, vol. doi:10.1016/j.jenvman.2007.06.024, 2008.

[5] K. Topouzelis, V. Karathanassi, P. Pavlakis, and D. Rokos, "Detection and discrimination between oil spills and look-alike phenomena through neural networks," *ISPRS Journal of Photogrammetry and Remote Sensing*, vol. 62, pp. 264-270, 2007.

[6] C. A. Topaloglou, T. K. Alexandridis, E. Lazaridou, and G. C. Zalidis, "Assessment of GlobWetland products for monitoring aquacultures in a greek coastal wetland," presented at European Space Agency, (Special Publication) ESA SP, 2006.

[7] T. K. Alexandridis, C. A. Topaloglou, E. Lazaridou, and G. C. Zalidis, "The performance of satellite images in mapping aquacultures," *Ocean and Coastal Management*, vol. doi: 10.1016/j.ocecoaman.2008.06.002, 2008.

[8] T. K. Alexandridis, K. Perakis, and N. Silleos, "Flood monitoring using ERS-1 SAR imagery and DEM," in *Proceedings of 1st IFAC Workshop on Control Applications and Ergonomics in Agriculture*. Athens, Greece, 1998.

[9] M. Chakraborty, S. Panigrahy, and S. A. Sharma, "Discrimination of rice crop grown under different cultural practices using temporal ERS-1 synthetic aperture radar data," *ISPRS Journal of Photogrammetry and Remote Sensing*, vol. 52, pp. 183-191, 1997.

[10] R. P. Shrestha, "Relating soil electrical conductivity to remote sensing and other soil properties for assessing soil salinity in northeast Thailand," *Land Degradation and Development*, vol. 17, pp. 677-689, 2006.

[11] R. Evans and D. M. Carroll, "Radar images for soil survey in England and Wales," *ITC Journal*, vol. 1, pp. 88-93, 1986.

[12] A. Burini, A. Minchella, and D. Solimini, "SAR in agriculture: Sensitivity of backscattering to grapes," presented at International Geoscience and Remote Sensing Symposium (IGARSS), 2005.

[13] E. Chen, Z. Li, Y. Pang, and X. Tian, "Quantitative evaluation of polarimetric classification for agricultural crop mapping," *Photogrammetric Engineering and Remote Sensing*, vol. 73, pp. 279-284, 2007.

[14] S. E. Franklin, "Topographic dependence of synthetic aperture radar imagery," *Computers & Geosciences*, vol. 21, pp. 521-532, 1995.

[15] T. Bayer, R. Winter, and G. Schreier, "Terrain influences in SAR backscatter and attempts to their correction," *IEEE Transactions on Geoscience and Remote Sensing*, vol. 29, pp. 451-462, 1991.

[16] K. Blyth, "An assessment of the capabilities of the ERS satellites' active microwave instruments for monitoring soil moisture change," *Hydrology and Earth System Sciences*, vol. 1, pp. 159-174, 1997.

[17] D. B. Michelson, "ERS-1 SAR backscattering coefficients from bare fields with different tillage row directions," *International Journal of Remote Sensing*, vol. 15, pp. 2679-2685, 1994.

[18] P. S. Wright, "Soils in Bedfordshire 1: Sheet TL14 (Biggleswade)," *Soil Survey Record No. 112*, 1987.

[19] E. A. Edmonds and C. H. Dinham, "Geology of the country around Huntingdon and Biggleswade.," *Memoir for 1:50 000 geological sheet 112, Geological Survey of UK*, 1965.

[20] M. C. Dobson, F. T. Ulaby, and L. E. Pierce, "Land-cover classification and estimation of terrain attributes using synthetic aperture radar," *Remote Sensing of Environment*, vol. 51, pp. 199-214, 1995.

[21] H. Laur and J. I. Sanchez, "The ERS SAR products: Their generation, their quality and their calibration," *European Space Agency, (Special Publication) ESA SP*, pp. 19-24, 1997.

[22] J. W. Trevett, *Imaging radar for resources surveys*: Chapman and Hall, 1986.

[23] M. Benallegue, O. Taconet, D. Vidal-Madjar, and M. Normand, "The use of radar backscattering signals for measuring soil moisture and surface roughness," *Remote Sensing of Environment*, vol. 53, pp. 61-68, 1995.

[24] T. Hess, "A microcomputer scheduling program for supplementary irrigation," *Computers and Electronics in Agriculture*, vol. 15, pp. 233-243, 1996.